

UDK 535.37

## Annealing and Doping Concentration Effects on $Y_2O_3: Sm^{3+}$ Nanopowder Obtained by Self-Propagation Room Temperature Reaction

S. Čulubrk, V. Lojpur, V. Đordjević, M. D. Dramićanin<sup>\*)</sup>

Vinča Institute of Nuclear Sciences, University of Belgrade, P.O. Box 522, Belgrade, Serbia

---

### Abstract:

*In this report, structure, morphology and luminescence of  $Y_2O_3:Sm^{3+}$  nanoparticles prepared by self-propagating room temperature reaction are presented. This new, simple and cost effective synthesis allows obtaining desired phase composition by mixing appropriate amounts of yttrium and samarium nitrates together with sodium hydroxide. A set of samples is prepared with different  $Sm^{3+}$  concentrations (0.1, 0.2, 0.5, 1 and 2 at %) in order to observe changes of luminescence properties. Also, effects of post synthesis annealing at several temperatures (600 °C, 800 °C and 1100 °C) are analyzed. For all samples X-ray diffraction showed that powders have cubic bixbyite structure (Ia-3), and TEM analysis showed particles of less than 100 nm. Luminescence emission spectra clearly show peaks characteristic for electronic spin-forbidden transition of  $Sm^{3+}$  ions  $^4G_{5/2} \rightarrow ^6H_{5/2}$ ,  $^6H_{7/2}$  and  $^6H_{9/2}$  centered at 578, 607 and 654 nm, respectively. Emission lifetime values decrease with  $Sm^{3+}$  ion concentration increment, from 1.94 ms for 0.1 at% to 0.97 ms for 2 at%. In addition, enlargement of lifetime value is observed when thermal treatment is done at the highest temperature due to the elimination of luminescence quenching species from the surface of particles.*

**Keywords:** Luminescence,  $Y_2O_3$ ,  $Sm^{3+}$ , Self-propagating room temperature.

---

### 1. Introduction

In a past few decades, phosphor materials have become highly significant because of their wide application in various optoelectronic devices [1]. Particularly, there is a considerable interest in studies of ultrafine and nanocrystalline oxide and non-oxide materials doped with rare- earth (RE) ions in terms of fundamental research and applications in display devices and lamps, biomedical multicolor imaging, scintillators, high-power solid-state lasers, etc [2-4]. Among them, sesquioxides represent well-recognized host matrices because of the good chemical stability and thermal conductivity as well as high light output [5]. Yttrium-oxide ( $Y_2O_3$ ) is due to its low vibrational energy, optical band transparency (0.20-8  $\mu m$ ), large refractive index ( $> 1.9$ ), high energy band gap (5.8 eV), high melting point (2450 °C) and high phonons frequency, which favors the radiation emission and prevents non-radiation relaxation excitation levels, excellent choice for host material [6]. It also facilitates easy rare-earth ion substitution and enables luminescent characteristics of a high efficiency. Trivalent RE ions such as  $Eu^{3+}$ ,  $Sm^{3+}$ ,  $Ce^{3+}$ ,  $Dy^{3+}$ ,  $Er^{3+}$ ,  $Tb^{3+}$ ,  $Ho^{3+}$  possess partially filled 4f orbitals with characteristics energy levels from which optical transitions occurs on different energies

---

<sup>\*)</sup> Corresponding author: dramicanin@vinca.rs

getting in that way various emission colors [7]. For example,  $Y_2O_3$  doped with  $Eu^{3+}$ ,  $Tb^{3+}$  or  $Tm^{3+}$  gives red, green and blue emissions, respectively. RE ions are particularly suitable for the photoluminescence processes, since they have long excited state lifetime and good chemical durability and therefore  $Y_2O_3$  doped with RE ions represents a particularly good combination for obtaining efficient luminescent materials.

Traditionally, oxide-based phosphors were prepared using solid-state reaction method which includes a mechanical mixing of precursor oxides followed by a ball-milling and calcination [8]. This kind of procedure at high processing temperature leads to the non-homogeneity of a sample, wide size distribution and imprecise control of cation stoichiometry. Some of these shortcomings can be overcome using soft chemical routes that allow obtaining smaller particles e.g. in the nanometer range. Physical properties of the host materials with nanometer dimensions are remarkably different from micron-scale materials and, therefore, optical properties of the dopant ions may be significantly different. For example, reduction in particle size enable modifications of emission lifetimes, control of spatial distribution of dopant ions that results in amplification of a specific wavelength and efficient transmission of energy. Nanomaterials can effectively reduce unwanted light scattering when their size is far smaller than the wavelength of the incident light. Therefore, the synthesis methods for obtaining nanoparticles with precisely defined structure and morphology is of crucial importance for the improvement of materials functional characteristics. Sesquioxide nanopowders are excellent starting materials for preparation of luminescent ceramics [1, 9]. It has been shown that the reduction of the grain size of starting powder precursor to the nano level enables production of ceramics with higher fracture toughness and hardness [10], and also lowers the sintering temperature in comparison with those produced from conventional precursors [11].

Yttrium-oxide is one of the most explored hosts for the preparation of up and down conversion luminescent materials. So, methods for its production are numerous like spray pyrolysis [12], sol-gel [13], combustion [14], hydrothermal synthesis [15], polyol method [16], precipitation and co-precipitation [17], reverse micelle synthesis [18], etc. Depending on the rare earth dopant both up and downconversion can be obtained using the same synthesis procedure. One of examples is spray pyrolysis where doping with  $Eu^{3+}$  provided down-converted red emission [19], and  $Ho^{3+}$  and  $Tm^{3+}$  gave up-converted green and blue emission, respectively [20]. Besides all of these different methods, there is no report of obtaining  $Y_2O_3$  by self-propagating room temperature (SPRT) method. SPRT known as very simple, extremely time-effective and low-cost synthesis that is particularly suitable for producing nanocrystalline materials. So, in this paper we used this method in order to prepare nanosized powder of  $Y_2O_3$  doped with different  $Sm^{3+}$  ion concentration and to examine its effects on photoluminescence properties.

## 2. Experimental details

### 2.1. Sample preparation

Yttrium oxide powders doped with different concentration of  $Sm^{3+}$  (0.1, 0.2, 0.5, 1 and 2 at %) were synthesized *via* self-propagating room temperature reaction. Starting chemicals  $Y(NO_3)_3 \cdot 6H_2O$  and  $Sm(NO_3)_3 \cdot 6H_2O$  (both Alfa Aesar, 99.9% purity) previously stoichiometry calculated were mixed with sodium hydroxide (NaOH). Reaction proceeds at room temperature after the mixture of reactants are mechanically activated by hand mixing in alumina mortar for 5-7 min. After being exposed to air for 3h the mixture is washed in a centrifuge at 3800 rpm for 10 min. This procedure was performed five times with distilled water and two times with ethanol in order to eliminate  $NaNO_3$ . After that, material was dried in a hothouse for 12h at  $70^\circ C$ . In order to achieve target crystal structure powder was thermally treated at 600, 800 and  $1100^\circ C$  for 1 h. Procedure is schematically shown at Fig 1.

## 2.2. Instruments and measurements

Crystal structure was identified by X-ray powder diffraction on a Rigaku SmartLab system operating with Cu  $K_{\alpha 1,2}$  radiation at 40 mA and 30 kV. Data were taken in the  $2\theta$  range from  $15^\circ$  to  $100^\circ$  using continuous scan of  $0.7^\circ/s$ . The microstructure of powders was investigated with transmission electron microscopy JEOL-JEM 2100 LaB6 operated at 200 kV. Photoluminescence measurements including excitation and emission spectra and lifetime were recorded on the Fluorolog-3 Model FL3-221 (Horiba Jobin-Yvon), under excitation light of a 450W Xenon lamp.

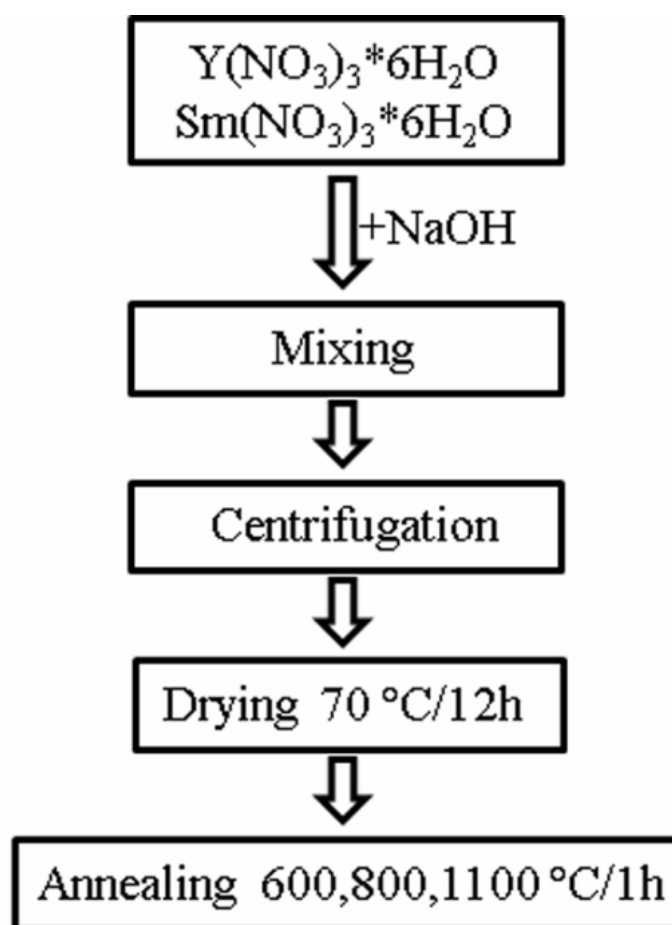


Fig. 1. Schematic procedure of SPRT method

## 3. Results and discussion

### 3.1. X-ray diffraction analysis (XRD)

The powders obtained via SPRT method exhibit cubic crystal structure, with space group  $Ia-3$ , that corresponds to the  $Y_2O_3$  (PDF 00-025-1200). This structure has two crystallographically non-equivalent sites for  $Y^{3+}$  ions that can be substituted with  $Sm^{3+}$  dopant ions: non-centrosymmetric  $C_2$  and centrosymmetric  $S_6$  ( $C_{3i}$ ). Due to their lower symmetry and greater abundance in the structure, lanthanoide ions preferably accommodates in the  $C_2$  site. One representative XRD spectrum is shown in Fig. 2 and corresponds to the  $Y_2O_3: 2 \text{ at\% } Sm^{3+}$  sample that is calcined at  $1100^\circ C$  for 1h.

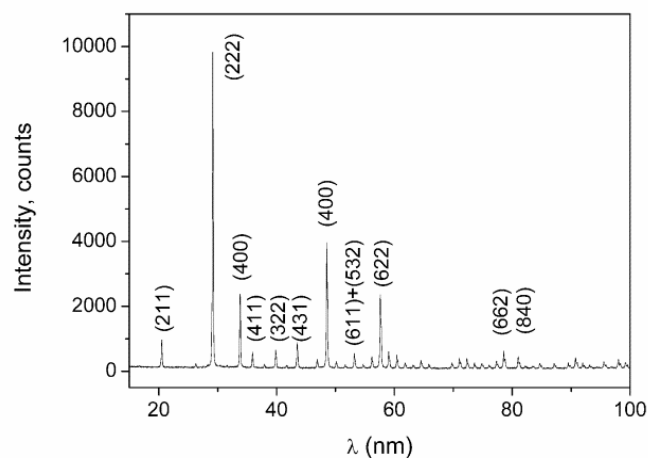


Fig. 2. XRD pattern of  $\text{Y}_2\text{O}_3$ : 2 at%  $\text{Sm}^{3+}$  calcined at 1100 °C for 1 h

### 3.2. Transmission electron microscopy (TEM)

TEM micrographs of  $\text{Y}_2\text{O}_3$  doped with 2 at%  $\text{Sm}^{3+}$  thermally treated at 1100 °C for 1 h are shown in Fig. 3. It can be clearly observed presence of agglomerates that are consisted of primary particles having the size around 100 nm (Fig. 3a). The selected-area electron diffraction (SAED) pattern presented in Fig. 3b confirmed that powder possesses polycrystalline nature.

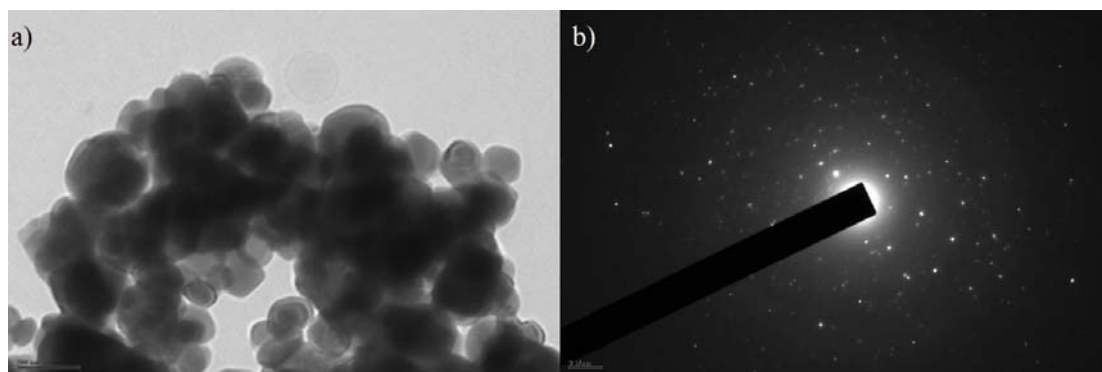
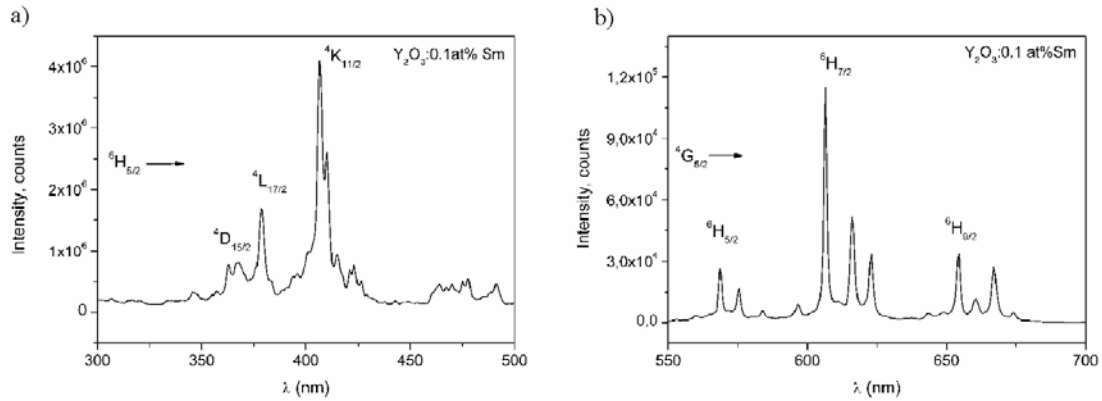


Fig. 3. TEM micrographs of  $\text{Y}_2\text{O}_3$ : 2 at%  $\text{Sm}^{3+}$  calcined at 1100 °C for 1 h

### 3.3. Luminescence properties

The  $\text{Sm}^{3+}$  ion with  $4f^6$  configuration has many energy levels that under the excitation, exhibit a red luminescence. Independently of  $\text{Sm}^{3+}$  concentration electronic transitions were the same for all samples. Photoluminescent excitation and emission spectra of sample  $\text{Y}_2\text{O}_3$  doped with 0.1 at%  $\text{Sm}^{3+}$  are presented in Fig 4 (a) and (b), and they are consisting from spectral features that are characteristic for  $\text{Sm}^{3+}$  emission from sesquioxides [5]. It can be seen that excitation spectra recorded in the range from 300–500 nm consist of lines at 363, 378 and 407 nm which can be assigned to the transition from the ground  $^6\text{H}_{5/2}$  level to  $^4\text{D}_{15/2}$ ,  $^4\text{L}_{17/2}$  and  $^4\text{K}_{11/2}$  levels, respectively. The emission spectrum is obtained by excitation of 406 nm at room temperature. Three emission bands in the visible region are observed which are assigned to the intra-4f-shell  $^4\text{G}_{5/2} \rightarrow ^6\text{H}_J$  transitions ( $J = 5/2, 7/2, 9/2$ ). The transition  $^4\text{G}_{5/2} \rightarrow ^6\text{H}_{5/2}$  includes three peaks at 568, 575 and 584 nm,  $^4\text{G}_{5/2} \rightarrow ^6\text{H}_{7/2}$  transition have peaks positioned at 596, 606, 616, 623 nm while  $^4\text{G}_{5/2} \rightarrow ^6\text{H}_{9/2}$  transition correspond peaks at 643, 654, 660, 667,

674 nm. The splitting of the emission manifolds and observed peak maxima are consequence of crystal field that acts on dopant ion located in the host matrix [21].



**Fig.4.** Excitation (a) and emission (b) spectra of  $\text{Y}_2\text{O}_3:0.1 \text{ at}\% \text{ Sm}^{3+}$  sample ( $\lambda_{\text{exc}} = 406 \text{ nm}$ )

The fluorescence decay curves along with lifetime values for  ${}^4\text{G}_{5/2}$  level of  $\text{Y}_2\text{O}_3:\text{Sm}^{3+}$  doped with different concentrations (0.1, 0.2, 0.5, 1 and 2 at %) are presented in Fig 5 (a and b, respectively). It can be observed that increasing concentration of dopant ions resulted in lower values of life time, so the greatest value (1.94 ms) was obtained for 0.1 at% Sm and the lowest value of lifetime (0.97 ms) for 2 at% Sm. Since the some of the fluorescence decay curves showed complex behavior (1 at%, 2 at% Sm) it was more appropriate to calculate an average lifetime values for all samples, using the following equation:

$$\tau_{\text{avg}} = \frac{\int_0^{\infty} tI(t) dt}{\int_0^{\infty} I(t) dt} \quad (1)$$

where  $I(t)$  represent the luminescence intensity at time  $t$  corrected for the background and the integrals are evaluated on a range  $0 < t < t_m$  where  $t_m \gg \tau_{\text{avg}}$ .

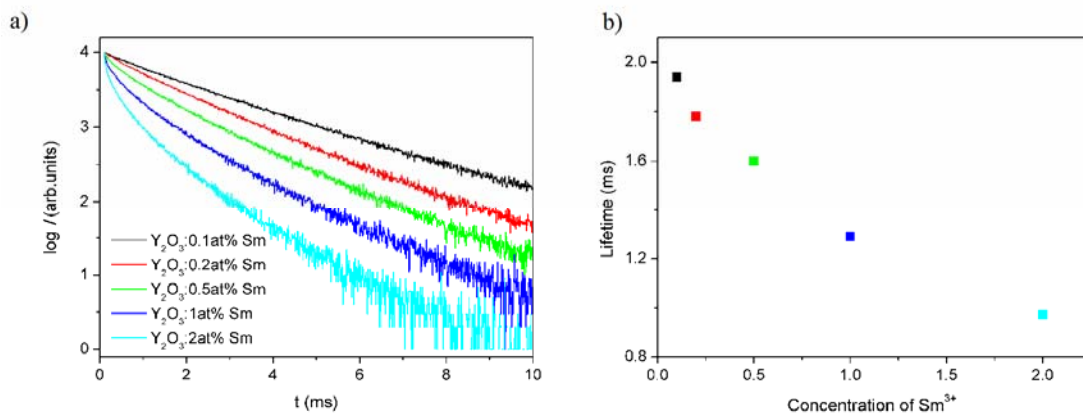


**Fig. 5.** The fluorescence decay curves (a) and lifetime values (b) of  $\text{Y}_2\text{O}_3:\text{Sm}^{3+}$

Luminescence efficiency is also observed in the function of various thermal treatment temperatures (600, 800 and 1100 °C) for sample  $\text{Y}_2\text{O}_3: 2 \text{ at}\% \text{ Sm}^{3+}$ . One can see that lifetime values are increased with elevation of temperature, so at 600 °C  $\tau_{\text{avg}}$  is 1 ms while at 1100 °C  $\tau_{\text{avg}}$  is 1.22 ms.

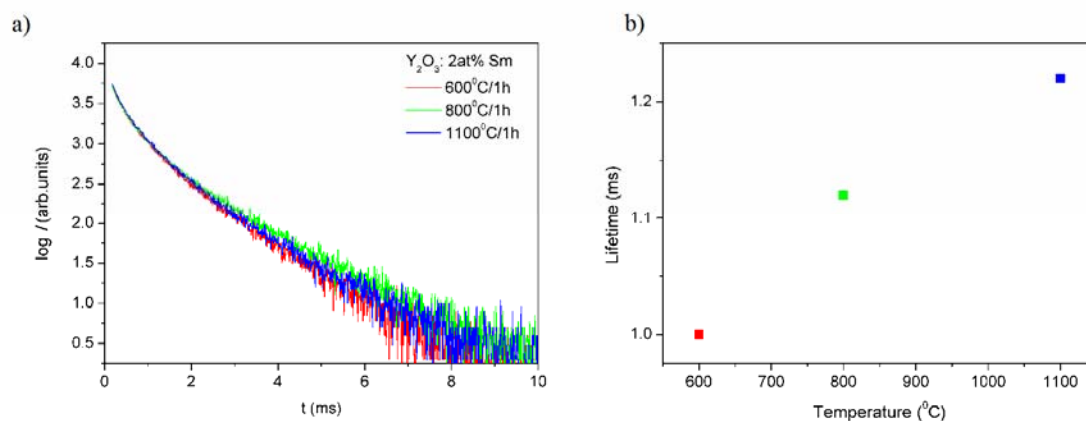


**Fig. 6.** The fluorescence decay curves (a) and lifetime values (b) of Y<sub>2</sub>O<sub>3</sub>: 2 at% Sm<sup>3+</sup> thermally treated at 600, 800 and 1100 °C for 1 h.

#### 4. Conclusion

Powders of yttrium oxide doped with different Sm<sup>3+</sup> concentration and thermally treated at various temperatures were successfully prepared by SPRT method. All samples possess appropriate phase composition and structure which is confirmed through XRD measurements. TEM micrographs showed that SPRT synthesis method ensure obtaining nanoparticles with polycrystalline nature with size below 100 nm. Emission spectra of all samples showed typical transitions of Sm<sup>3+</sup> ion and that lifetime values decrease with increasing its concentration. Influence of thermal treatment implies that a higher annealing temperature leads to the rising of lifetime values.

#### Acknowledgments

This research is financially supported by the Projects 45020 and 171022 of the Ministry of Science and Education of the Republic of Serbia.

#### 5. References

1. R.Krsmanovic, Z. Antic, M.G. Nikolic, M. Mitric, M.D. Dramicanin, *Ceram. Int.* 37 (2011) 525
2. E. Zych, M. Wawrzyniak, A. Kossek, J. Trojan-Piegza, L. Kepinski, *J. Alloy. Compd.*, 451 (2008) 591
3. A.Garcia-Murillo, C. Le Luyer, C. Dujardin, T. Martin, C. Garapon, C. Pedrini, J. Mugnier, *Nucl. Ins. Methods A*, 486 (2002) 81
4. H. Guo, X. Yang, T. Xiao, W. Zhang, L. Lou, J. Mugnier, *Appl. Surf. Sci.*, 230 (2004) 215
5. Radenka Krsmanović, Željka Antić, Barbora Bártoová and Miroslav D. Dramićanin, *J. Alloy. Compd.*, 505 (2010) 224
6. A. Martinez, J. Morales, L.A. Diaz-Tores, P. Salas, E. de la Rosa, J. Oliva, H. Desirena, *Mater. Sci. Eng B*, 174 (2010) 164
7. K.M. Nissamudeen, K.G. Gopchandran, *J. Alloy. Compd.* 490 (2010) 399
8. X. Hou, S. Zhou, T. Jia, H. Lin, H. Teng, *Physica B* 406 (2011) 3931

9. R.M. Krsmanović, Ž. Antić, B. Bártová, M.G. Brik, M.D. Dramićanin, Ceram. Int. 38, (2012) 1303
10. Dj. Veljović, G. Vuković, I. Steins, E. Palcevskis, P. S. Uskoković, R. Petrović, Dj. Janačković, Science of Sintering, 45 (2013) 233
11. W. Yan, N. Li, J. Tong, G. Liu, J. Xu, Science of Sintering 45 (2013) 165
12. W.N. Wang, W. Widiyastuti, T. Ogi, I. W. Lenggoro, K. Okuyama, Chemistry of Materials, 19 (2007) 1723
13. Q. Yanmin, G. Hai, J. Rare Earths 27 (2009) 406
14. D. L. Phan, M. H. Phan, N. Vu, T.K. Anh, S.C. Yu, Phys. Status Solidi, 201 (2004) 2170
15. M. K. Devaraju, S. Yin, T.Sato, Eur. J. Inorg. Chem., (29-30) (2009) 4441
16. M. A. Flores-Gonzales, G. Ledoux, S. Roux, K. Lebbou, P. Perriat, O. Tillement, J. Solid State Chem., 187 (2005) 989
17. J. Li, Y. Zhang, G. Hong, Y. Yu, J. Rare Earths, 26 (2008) 450
18. O. A. Graeve, J.O. Corral, Opt. Mater. 29 (2006) 24
19. K. Marinković, L. Mančić, L. S. Gomez, M. E. Rabanal, M. Dramićanin, O. Milošević, Opt. Mater., 32 (2010) 1606
20. V. Lojpur, M. G. Nikolić, L. Mančić, O. Milošević, M. D. Dramićanin, Opt. Mater., 35 (2012) 38
21. Ž. Andrić, M. D. Dramićanin, M. Mitrić, V. Jokanović, A. Bessière and B. Viana, Opt. Mater., 30 (2008) 1023

---

**Садржај:** У овом раду приказана су структурна, морфолошка и луминесцентна својства наночестица итријум-оксида допираног самаријумом, које су добијене самостално-пропагирајућом реакцијом на собној температури. Ова нова, једноставна и економична синтеза омогућава добијање честица жељене фазе, мешањем одговарајућих количина итријум- и самаријум-нитрата са натријум-хидроксидом. Сет узорка припремљен је са различитим концентрацијама самаријума (0,1, 0,2, 0,5, 1 и 2 ат%) како би се посматрале промене луминесцентних карактеристика. Такође, анализирани су и ефекти накнадног термичког жарања на температурама 600, 800 и 1100 °C. За све узорке рендгенска дифракција показала је да прахови поседују кубну биксбитну структуру (1а-3), а ТЕМ анализа је показала да честице имају величину испод 100 nm. Емисиони спектри показују карактеристичне пикове за јоне самаријума  ${}^4G_{5/2} \rightarrow {}^6H_{5/2}$ ,  ${}^6H_{7/2}$  и  ${}^6H_{9/2}$  који су центрирани на 578, 607 и 654 nm, респективно. Вредности времена живота повећавају се са смањењем концентрације самаријума од 1,94 ns за 0,1 ат% до 0,97 ns за 2 ат%. Поред тога, повећање времена живота примећено је на највишој температури због елиминације група са површине узорка које гасе луминесценцију.

**Кључне речи:** луминесценција,  $Y_2O_3$ ,  $Sm^{3+}$ , Самостално-пропагирајућа реакција на собној температури

---